Journal of the Serbian Society for Computational Mechanics / Vol. 16 / No. 2, 2022 / pp 67-86
(10.24874/jsscm.2022.16.02.05)

UNSTEADY NUMERICAL INVESTIGATION OF FERROFLUID FORCED CONVECTION OVER A DOWNWARD STEP CONTAINING A ROTATING FINNED CYLINDER

Meriem Toumi[1]*, Mohamed Bouzit[1], Abderrahim Mokhefi[2], Djamila Derbal[1]

[1] Laboratory of Maritime Sciences and Engineering LSIM Faculty of Mechanical Engineering, University of Science and Technology of Oran, Mohamed Boudiaf, El Mnaouar, B.P.1505, 31000, Oran, Algeria
e-mail: meriem.toumi@univ-usto.dz, bouzit_mohamed@yahoo.fr, djamila.derbal@univ-usto.dz
2 Mechanics, Modeling and Experimentation Laboratory L2ME, Faculty of Sciences and Technology, Bechar University B.P.417, 08000, Bechar, Algeria
e-mail: abderrahim.mokhefi@univ-bechar.dz
**corresponding author*

Abstract

The unsteady investigation of ferrofluid flow forced convection over a downward step containing a rotating finned cylinder is conducted numerically. The dimensionless partial differential equations of conservation equations for mass, momentum and energy and the boundary conditions associated with them are solved by using the finite element method. Two control parameters are used, the angular velocity Ω (-5, -3, -1, 0, 1, 3, 5) and the Reynolds number Re (10, 20, 50, 100), and their effect as a function of time on flow characteristics and heat transfer is presented. To understand how the rotation of the finned cylinder and Reynolds number affects the heat transfer and fluid flow characteristics, an analysis is made and the results obtained are presented qualitatively by the streamlines and the isotherms and quantitatively by calculating the average and local Nusselt number. It has been observed that the rotation of the finned cylinder enhanced heat transfer significantly. A difference of 177.33% improvement is observed between a rotational speed of a finned cylinder (Ω = -5) in the present paper and that of a cylinder without fin (Ω = 25) in the reference paper.

Keywords: Rotating finned cylinder, heat transfer, nanofluid, forced convection, downward step.

1. Introduction

Asymmetrical sudden expansion such as downward steps can be found in various engineering applications such as combustion chambers, heat exchangers and fluid machines etc. Downward steps or Backward-facing steps (BFS) are widely used as references in numerical simulations due to their simplicity. Several numerical and/or experimental investigations have been performed using BFS geometries to study the characteristics of the heat transfer and the ferrofluid flow. Moosavi et al. (2021) developed a numerical investigation using the step length of the BFS as a control parameter. The results showed that as the step length down of BFS increases, the average

Nusselt number also increases. Nath and Krishnan (2019) and Lv (2019) proceeded by adding nanoparticles to numerically study the nanofluid flow characteristics and heat transfer quality in a backward facing step. iIt was shown that the nanoparticles inserted into the base fluid increase the average Nusselt number value. Hillo et al. (2020) carried out experimental work to analyze the difference between two nanofluids, CuO-EG and MgO-EG. The results revealed that the heat transfer rate for the CuO-EG nanofluid is higher than that for the MgO-EG nanofluid. In the studies by Kherbeet (2012), Mobadersani and Rezavand Hesari (2020), Al-Aswadi et al. (2010), Turkyilmazoglu (2014) and Selimefendigil and Öztop (2013), the aim was to show if the use of nanofluid affects the heat transfer in a backward facing step. The results revealed that the value of the average Nusselt number rises with increasing nanoparticles volume fraction. When using SiO_2 nanoparticle, the quality of heat transfer is elevated. It is also found that when the diameter of nanoparticles decreases, the Nusselt number increases. Between Cu and TiO_2, the nanofluid containing Cu nanoparticles has the highest heat transfer rate but it is lowest when using TiO_2 nanoparticles. Numerical simulation of laminar nanofluid forced convection on a backward step was carried out by Selimefendigil and Öztop (2015) and (2018a). In their studies, it was mentioned that the increase in heat transfer for a fluid containing nanoparticles is highest compared to water as fluid base. The type of nanoparticles used, and the particle shape, have significant impact on the characteristics of nanofluid flow and on the heat transfer quality. In addition, it was observed that with increase in the Reynolds number value, the heat transfer rate increases. Hussain and Ahmed (2019) analyzed the effect of Fe_3O_4-H_2O ferrofluid by forced convective flow on a BFS containing a rotating cylinder in the presence of magnetic field with inclination. This paper is the reference of our numerical investigation. The authors observed that when the cylinder rotates counterclockwise, the heat transfer rate improves. Toumi et al. (2022) used numerical simulations to study the forced convection of a laminar ferrofluid flow in a backward facing step containing a finned cylinder with different fin position. This study showed that adding a fin on the cylinder significantly affects the quality of the heat transfer.

A recent research study is of great interest for further study of the influence of rotational speed on the heat transfer and on nanofluid flows characteristics around cylindrical obstacle set in rotation with different convection mode. These areas are of operational use such as rotating tube heat exchangers. Selimefendigil and Öztop (2014) and (2020) and Kumar and Dhiman (2012) showed that when the cylinder rotates clockwise, more flow is entrained in the wake of the cylinder. On the other hand, when a circular cylinder is used, the maximum Nusselt value is improved up to 155% compared to the case without a cylinder. This is particularly the case for clockwise rotation where the increase in the local Nusselt value is 244% compared to the non-rotating cylinder case. The maximum Nusselt values increase with the Reynolds number.

Several other studies investigated the effect of rotating cylinder on the thermal and hydrodynamic characteristics in cavities, according to references in Rahman et al. (2014), Yang et al. (2019), Costa and Raimundo (2010), Roslan et al. (2012) and Selimefendigil and Öztop (2018b). It was found that the presence of nanoparticles causes a stability of heat transfer which is disturbed for higher values of the Rayleigh number due to the mixing of the flows inside the cavity. The overall heat transfer rate is strongly dependent on the rotation speed of the cylinder; it is small if the rotation speed is low. The strength of the flow circulation significantly increases with higher nanoparticle concentration and faster negative rotation. The average Nusselt number is higher when the rotation is counterclockwise, and it is lower in the stationary cylinder configuration. Sufyan et al. (2015) studied numerically the 2D laminar nanofluid flow and heat transfer by forced convection through a rotating cylinder. For the value of the dimensionless rotation rate used and for the range of Prandtl numbers between 0.7 and 67, it was concluded that under the effect of rotation, the heat transfer rate is high for all Prandtl numbers. In the numerical study by Shirani et al. (2021), four rotating cylinders were introduced in a square cavity filled with the nanofluid of water-Cu, the Richardson number values were between 0.1 and 10, the

nanoparticle concentration ϕ was between 0 and 0.03 and Reynolds number values were between 86.2 and 862. They declared that with increasing nanoparticle concentration and Reynolds number, the Nusselt number increased. They also observed that under the impact of buoyancy forces on the flow, the effect of nanoparticles is less pronounced as the Richardson number increases. Some researchers, namely Ikhtiar et al. (2019), Yoon et al. (2018), Sarkar et al. (2016) and Xie and Xi (2022), have studied the fluid flow characteristics and the quality of heat transfer using a rotating cylinder. They mentioned that forced convection heat transfer affects the cylinder surface, while the average Nusselt number increase when the value of the Reynolds number is high and the flow instability has a positive effect on the heat transfer. Selimefendigil and Öztop (2015) conducted a numerical study using mixed convection in a backward facing step in which a rotating cylinder was inserted to a nanofluid. A commercial solver based on finite element method was used to solve partial differentials equations. The improved heat transfer is obtained for certain parameter combinations, and it was shown that linear increase in the heat transfer enhancement exists with increasing volume fraction of the nanoparticles and Reynolds number. Moreover improvement was obtained for certain angular velocities of the cylinder. Xie et al. (2017) investigated the effect of the vortex structure on heat transfer enhancement in a backward facing step geometry. They studied the characteristics of nanofluid laminar flow, heat transfer quality and impact of the vortex structure. It was found that the instability of flow appeared downstream of the primary recirculation zone, which generated many vortices that had a positive effect.

As mentioned above, previous studies have provided sufficient guidance for new investigations of heat transfer and nanofluid flow characteristics of various types of convection around rotating bodies. Many current studies deal with these problems using circular obstacle.

The present study, which has not been done before, adds new knowledge by addressing the nanofluid flow and heat transfer properties of a rotating finned cylinder. The streamlines contours, the isotherm profiles and the average and local Nusselt number are used to present the results.

2. Physical configuration of geometry

2.1. Description of physical model

An unsteady 2D numerical analysis of nanofluid flow by forced convection on a backward facing step containing a rotating finned cylinder is studied and physical configuration with boundary conditions is shown in Fig. 1. The step length of the backward facing step is H and the height of horizontal duct is 2H. Ω is adimensional angular rotational velocity of finned cylinder. The radius of cylinder is (D = H), the center cylinder position is (4H, H) and the fin length is 0.2H. At the duct inlet the velocity is u = u0 and v = 0 and at the duct outlet, the gradient of all variables in x-direction are equal to zero, Tc is the low temperature of the ferrofluid and Th represent the high temperature of the bottom wall. The value of Prandtl number base fluid is equal to 6.2 and constant values of the thermophysical properties of H2O and Fe_3O_4 are presented in Table 1. The energy equation is modelled without considering the viscous dissipation and Joule heating and one phase ferrofluid model is used.

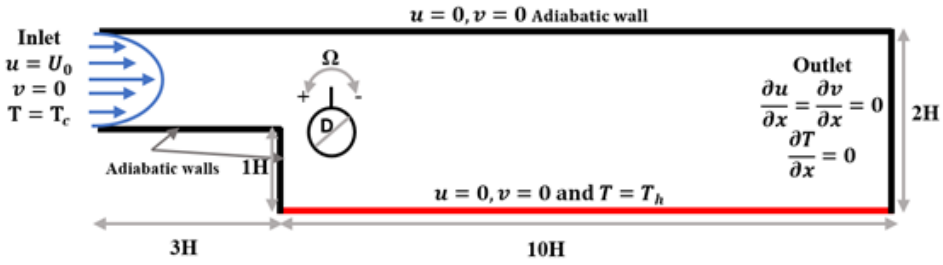

Fig. 1. Backward facing step geometry containing a rotating finned cylinder.

	ρ [Kg/m^3]	Cp [J.Kg^{-1}. K^{-1}]	k [W/m.K]
H_2O	997.1	4179	0.613
Fe_3O_4	5200	670	6

Table 1. Properties of ferrofluid (Fe_3O_4) and base fluid (Distilled Water), [Hussain and Ahmed 2019].

3. Mathematical equations

3.1. Dimensional form of instantaneous equations

The forced convective flow and heat transfer was modeled by instantaneous partial differential equations of the mass conservation, momentum, energy and streamlines function as follows:

$$\frac{\partial u}{\partial x} + \frac{\partial v}{\partial y} = 0 \tag{1}$$

$$\rho_{nf}\left[\frac{\partial u}{\partial t} + u\frac{\partial u}{\partial x} + v\frac{\partial u}{\partial y}\right] = -\frac{\partial p}{\partial x} + \mu_{nf}\left(\frac{\partial^2 u}{\partial x^2} + \frac{\partial^2 u}{\partial y^2}\right) \tag{2}$$

$$\rho_{nf}\left[\frac{\partial v}{\partial t} + u\frac{\partial v}{\partial x} + v\frac{\partial v}{\partial y}\right] = -\frac{\partial p}{\partial y} + \mu_{nf}\left(\frac{\partial^2 v}{\partial x^2} + \frac{\partial^2 v}{\partial y^2}\right) \tag{3}$$

$$\frac{\partial T}{\partial t} + u\frac{\partial T}{\partial x} + v\frac{\partial T}{\partial y} = \alpha_{nf}\left(\frac{\partial^2 T}{\partial x^2} + \frac{\partial^2 T}{\partial y^2}\right) \tag{4}$$

3.2. Dimensional boundary conditions

The duct inlet, x-direction velocity $(u = u_0, v = 0)$ and cold temperature $T = T_c$.

The bottom wall, no-slip velocity condition $(u = 0, v = 0)$ and hot temperature $T = T_h$.

The duct outlet, $\frac{\partial u}{\partial n}=\frac{\partial v}{\partial n}=0$, $\frac{\partial T}{\partial n}=0$.

Other walls are adiabatic and the velocity is no-slip. $(u=0, v=0)$ and $\frac{\partial T}{\partial n}=0$.

Finned cylinder is adiabatic $\frac{\partial T}{\partial n}=0$.

n is the surface normal direction coinciding with the x axis at the outlet.

Finned cylinder velocity components: $u=-\omega(y-y_0)$ and $v=\omega(x-x_0)$.

3.3. Dimensionless form of instantaneous equations

To obtain the dimensionless equations (6)-(10) the following scales are used:

$$X=\frac{x}{H}\quad U=\frac{u}{U_0}\quad \theta=\frac{T-T_c}{T_h-T_c}\quad \mathrm{Pr}=\frac{\mu_f Cp_f}{\kappa_{nf}}\quad \mathrm{Re}=\frac{\rho_f H U_0}{\mu_f}$$

$$Y=\frac{y}{H}\quad V=\frac{v}{U_0}\quad P=\frac{p}{\rho_{nf}U_0^{\,2}}\quad \tau=\frac{tU_0}{H}$$

Dimensionless *instantaneous* system obtained is:

$$\frac{\partial U}{\partial X}+\frac{\partial V}{\partial Y}=0 \tag{5}$$

$$\frac{\partial U}{\partial \tau}+U\frac{\partial U}{\partial X}+V\frac{\partial U}{\partial Y}=-\frac{\partial P}{\partial X}+\frac{1}{\mathrm{Re}}\frac{\rho_f}{\rho_{nf}}\frac{\mu_{nf}}{\mu_f}\left(\frac{\partial^2 U}{\partial X^2}\frac{\partial^2 U}{\partial Y^2}\right) \tag{6}$$

$$\frac{\partial V}{\partial \tau}+U\frac{\partial V}{\partial X}+V\frac{\partial V}{\partial Y}=-\frac{\partial P}{\partial Y}+\frac{1}{\mathrm{Re}}\frac{\rho_f}{\rho_{nf}}\frac{\mu_{nf}}{\mu_f}\left(\frac{\partial^2 V}{\partial X^2}\frac{\partial^2 V}{\partial Y^2}\right) \tag{7}$$

$$\frac{\partial \theta}{\partial \tau}+U\frac{\partial \theta}{\partial X}+V\frac{\partial \theta}{\partial Y}=\frac{\alpha_{nf}}{\alpha_f}\frac{1}{\mathrm{Re}\times\mathrm{Pr}}\left(\frac{\partial^2 \theta}{\partial X^2}+\frac{\partial^2 \theta}{\partial Y^2}\right) \tag{8}$$

3.4. Dimensionless Boundary conditions

The duct inlet, x-direction velocity is $(\mathrm{U}=\mathrm{U}_0, \mathrm{V}=0)$ and cold temperature is $\theta=0$.

The bottom wall, no-slip velocity condition $(\mathrm{U}=0, \mathrm{V}=0)$ and hot temperature is $\theta=1$.

The duct outlet, $\frac{\partial U}{\partial X}=\frac{\partial V}{\partial X}=0$ and $\frac{\partial \theta}{\partial X}=0$.

Other walls are adiabatic and the velocity is no-slip. $U=V=0$ and $\frac{\partial \theta}{\partial n}=0$.

Finned cylinder is adiabatic $\partial\theta/\partial\mathrm{n}=0$.

n is the surface normal direction coinciding with the x axis at the outlet.

Finned cylinder velocity components: $U = -\Omega\left(Y - Y_0\right)$ and $V = \Omega\left(X - X_0\right)$.

3.5. Thermophysical properties of nanofluid

The subscript 'p' represents the property of solid ferromagnetic particles.

Density $$\rho_{nf} = (1-\phi)\rho_f + \phi\rho_p \tag{9}$$

Thermal diffusivity $$\alpha_{nf} = \frac{\kappa_{nf}}{\rho_{nf} Cp_{nf}} \tag{10}$$

Specific heat $$(\rho Cp)_{nf} = (1-\phi)(\rho Cp)_f + \phi(\rho Cp)_p \tag{11}$$

Thermal conductivity $$\frac{\kappa_{nf}}{\kappa_f} = \frac{\kappa_p + 2\kappa_f - 2\phi(\kappa_f - \kappa_p)}{\kappa_p + 2\kappa_f + \phi(\kappa_f - \kappa_p)} \tag{12}$$

Thermal expansion coefficient $$(\rho\beta)_{nf} = (1-\phi)(\rho\beta)_f + \phi(\rho\beta)_p \tag{13}$$

Dynamic viscosity $$\mu_{nf} = \frac{\mu_f}{(1-\phi)^{2.5}} \tag{14}$$

3.6. Average and local Nusselt number Computation

The Nusselt number describes the ratio of the thermal energy of convected fluid to the thermal energy conducted within the fluid. The Nusselt number is the temperature gradient at the surface. The efficiency of heat transfer is determined by the value of the average or local Nusselt number.

The local Nusselt number is determined over the heated bottom wall and the total length of the heated wall is L.

$$Nu = \frac{h_{nf} \times L}{\kappa_f} \tag{15}$$

The coefficient of heat transfer of nanofluid is h_{nf}.

$$h_{nf} = \frac{q_w}{T_h - T_c} \tag{16}$$

The heat flux on the heated wall is q_w.

$$q_w = -\kappa_{nf} = \frac{T_h - T_c}{L}\frac{\partial\theta}{\partial y}\Big|_{y=0} \tag{17}$$

$$Nu = \frac{\kappa_{nt}}{\kappa_{nf}}\left(\frac{\partial\theta}{\partial Y}\right) \tag{18}$$

$$Nu_{avg} = \frac{1}{L}\int_0^L Nu dX \tag{19}$$

3.7. The numerical method and mesh independence test

The computational domain of the backward has been discretized with unstructured elements. The weighted residual (Galerkin) of finite element method analysis is used to obtain the numerical solution of the dimensionless partial differential equations of the mass conservation (6), X-momentum (7), Y-momentum (8), energy (9) and Stream function (10), as well as the associated boundary conditions.

The sliding mesh technique realized for the unsteady case is based on the MRF method (multiple references frame method). In this technique, the information passes from the fixed domain to the mobile domain via an interpolation. We create separate regions in the mesh and when we solve the equations, we start by physically moving the section of the mesh at the beginning of each time step so that much of the mesh is stationary and there is a small coin-shaped region around the finned cylinder. The start of the temporal evolution of the thermal state in the duct was considered after the laminar flow regime becomes stationary. The grid containing the finned cylinder rotates at each time step and the interface between the two regions is recalculated. The problem with this approach is that a very small time step is used and the computation is very expensive and time consuming.

In order to optimize a mesh, it is necessary to start with one that is more or less coarse and then refine it until the parameter values are stabilized. Five grids were used to perform the mesh test in order to choose the optimal one, and we noticed that the values of Nu_avg and θ_avg had a negligible difference between the fourth and the fifth grid (see Table 2). We observe from Table 2 that from a grid of 92491 the results become independent of the mesh size. Therefore, this mesh size will be retained for use in future simulations.

The mesh independence test was performed at dimensionless time $\tau = 200$ for $Pr = 6.2$, $\phi = 0.04$, $Re = 100$ and $\Omega = 1$.

Number of e lements	7651	13479	42430	92491	157737
Computing time	15017 s. (4 h, 10 min, 17 sec)	20187 s. (5 h, 36 min, 27 sec)	35627 s. (9 h, 53 min, 47 sec)	47243 s. (13 h, 7 min, 23 sec)	60694 s. (16 h, 51 min, 34 sec)
$\boldsymbol{Nu_{avg}}$	4.231692	4.401572	4.427415	4.428125	4.428085
$\boldsymbol{\theta_{avg}}$	0.191634	0.138074	0.141773	0.141875	0.141652

Table 2. Mesh independence test.

A triangular unstructured mesh was used to discretize the computational domain. Many grids with different number of elements were tested (see Table 2) to choose the optimal mesh (92491 elements) to obtain accurate results and minimal computation time to perform the computations.

3.8. Validation

To validate the reliability of our numerical calculation, the average Nusselt number (Nu avg) was calculated as function as the angular velocity and compared to those found previously from Hussain and Ahmed 2019, thus the contours of the isotherms are presented for some values of the angular velocity. The validation is done using control parameters values: Reynolds number ($Re = 100$), nanoparticle concentration ($\phi = 5\%$) and Prandtl number ($Pr = 6.2$), as presented in Fig. 2. We can say that there is good agreement in the present work of validation compared with

the reference results. Therefore, our current research objective to study the effect of rotation of a finned cylinder can be achieved.

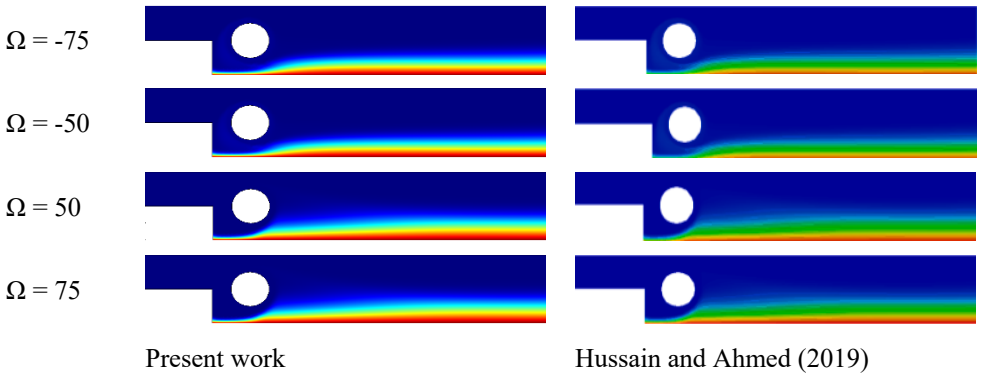

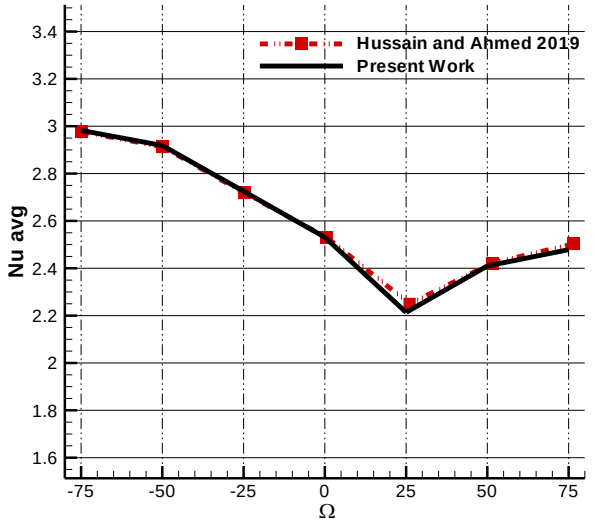

Fig. 2. Validation of results.

4. Results and discussion

The aim of this study was to investigate the impact of rotating finned cylinder on heat transfer quality improvement. An unsteady numerical investigation was performed to discover the effect of angular velocity as a control parameter. Various values for the angular velocity (-5, -3, -1, 0, 1, 3, 5) as well as Reynolds number (Re = 10, 20, 50 and 100) were used. Prandtl water number Pr = 6.2, and Grashof and Richardson numbers were very low. In the following, the results obtained through unsteady numerical calculations of ferrofluid heat transfer by forced convection in a backward facing step with a fin mounted on the cylinder are qualitatively presented by streamlines and isotherms in figures (3 – 6) and quantitatively by the average Nusselt number in figures (7 – 10) and the local Nusselt number in Figs. 11 and 12.

Qualitative results:

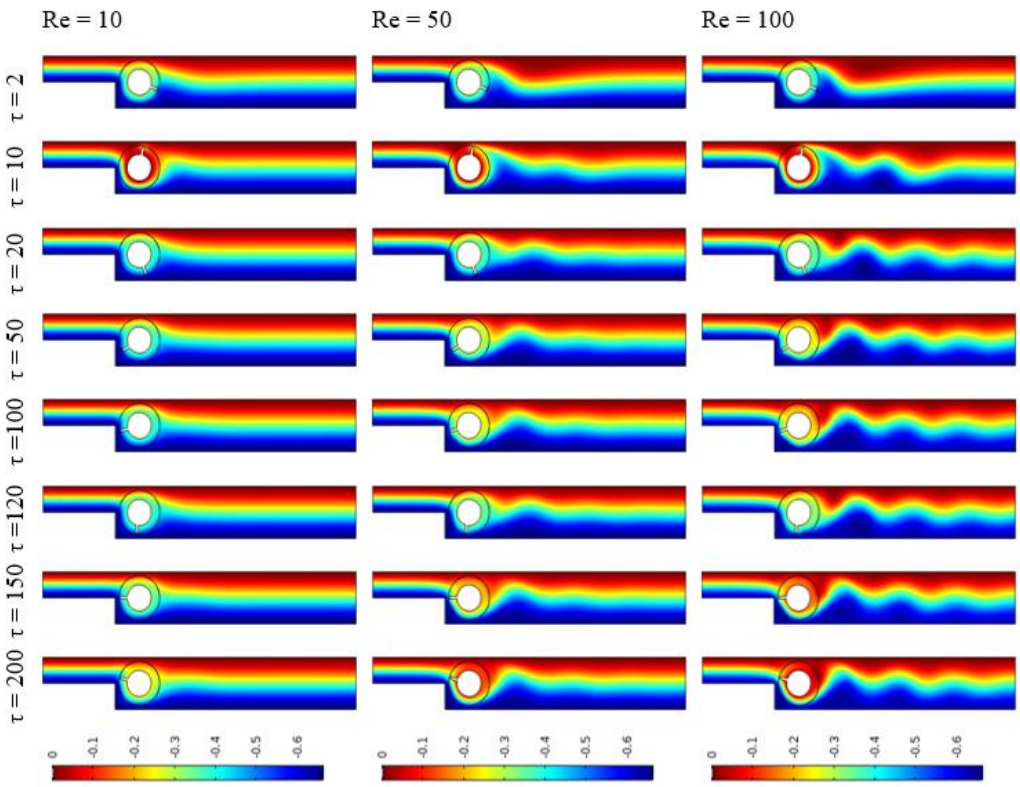

Fig. 3. Reynolds number impact on the streamlines at different times for Pr = 6.2, Ω = 1 and ϕ = 4%.

Fig. 3 shows the streamlines at eight instants with the variation of the Reynolds number (Re = 10, 50, 100) for the fixed values Pr = 6.2, Ω = 1 and ϕ = 4%. At low Reynolds numbers the viscosity is high, while the inertia is negligible, the flow motion is slow and no vortices exist, resulting in poor heat transfer. When the Reynolds number increases, the motion of the nanofluid becomes fast and vortices appear along the duct and near the bottom wall, as the inertial forces related to velocities are high. The number of vortices increases with increasing Reynolds number causing an enhancement of the forced convection which is most effective at Re = 100. The heat transfer becomes stable from the dimensionless time unit τ = 50.

The impact of the Reynolds number on the isotherms at different times from the interval τ [2 – 200] for Pr = 6.2, Ω = 1 and ϕ = 4% is presented in Fig. 4. It is clearly noticed that at Re = 10, the thickness of the thermal boundary layer along the bottom wall is large, which explains the poor forced convection. At this value of Reynolds number, the motion of the nanofluid is weak due to the viscous forces which are high, and the inertia forces related to velocities which are low. When the Reynolds number is equal to 100, the thickness of the thermal boundary layer along the bottom wall reduces and becomes thinner at Re = 100. This is due to the fact that the motion of the nanofluid is faster due to the increased inertial forces which cause the generation of vortices downstream of the obstacle causing an improvement in heat transfer. The location of the vortices causes a reduction in the thickness of the thermal boundary layer in the next to the bottom wall; these cold fluid vortices have an effect to improve the forced convection. For Reynolds number Re = 100, several vortices move one after the other behind the obstacle causing a good heat transfer. It is observed that in the areas where the vortices are generated next to the bottom wall,

the temperature fluctuates, the fluctuations are more intense when the Reynolds number value increases from 50 to 100 and the mixing of cold and hot fluid is improved. A stabilization of the heat transfer is noticed from the dimensionless time unit $\tau = 50$.

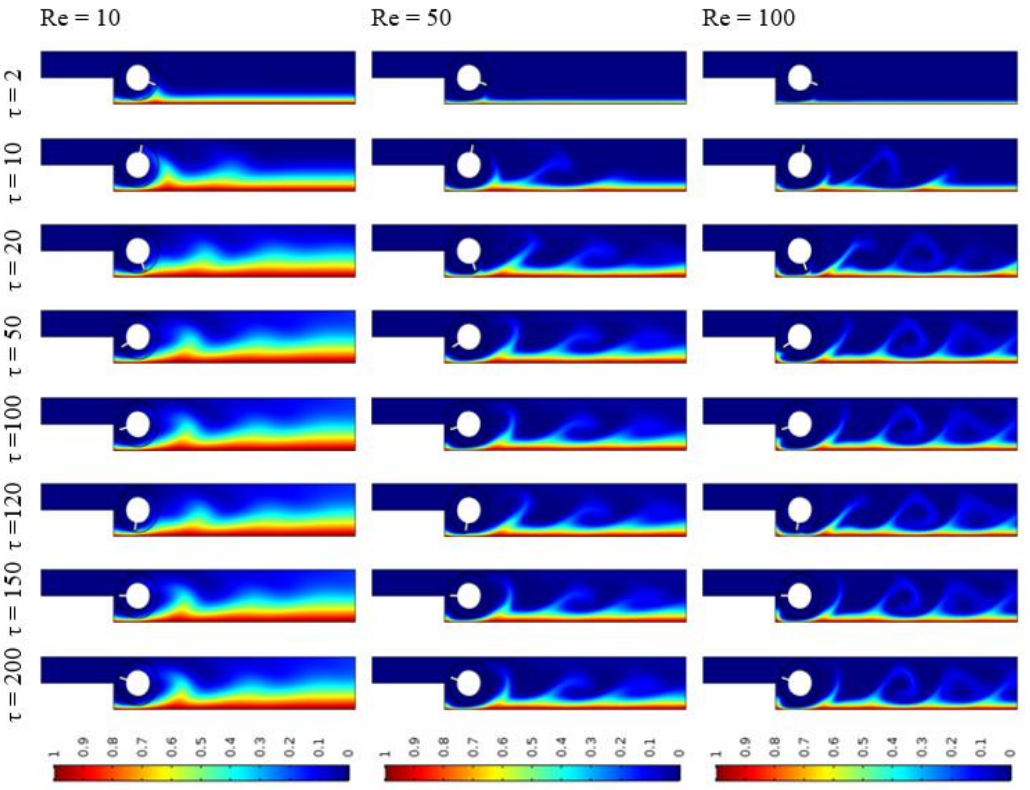

Fig. 4. Reynolds number impact on the isotherms at different times for Pr = 6.2, Ω = 1 and ϕ = 4%.

The contours of the streamlines at several instants of the unsteady numerical calculation to present the effect of the rotational speed of the finned cylinder are posed in Fig. 5. The chosen values of the rotational speed are (Ω = -3, 0, 5) and the fixed values are Pr = 6.2, Re = 100 with a nanoparticle concentration ϕ = 4%. A large flow rate of the nanofluid is observed when the obstacle is rotated for Ω = -3 and Ω = 5 which the heat transfer process improves. When the finned cylinder is rotating, a recirculation zone occurs, the location or region of this zone depends on the direction of rotation, which is just after the obstacle when the rotation is clockwise (Ω = -3). On the other hand it is far from the obstacle towards the end of the duct, when the finned cylinder rotates counterclockwise (positive rotation Ω = 5). For Ω = 0 (stationary obstacle), the flow rate is reduced and no vortex occurs, so the forced convection is reduced compared to the other values of the finned cylinder rotation speed.

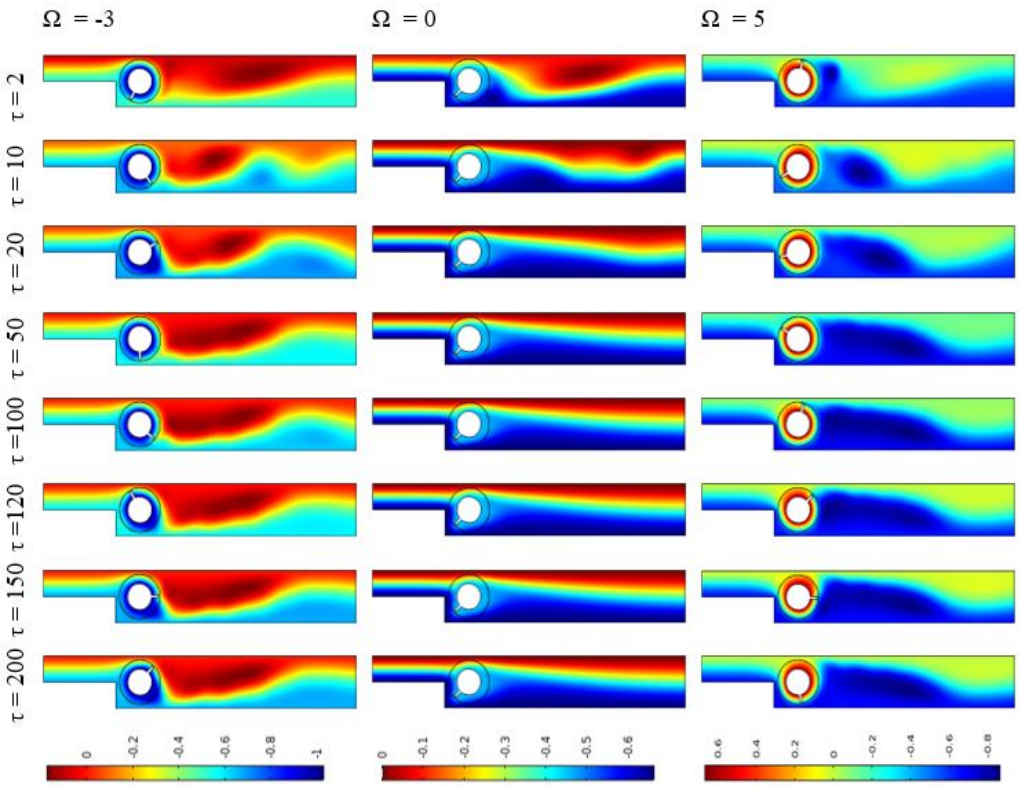

Fig. 5. Effect of the finned cylinder rotation (Ω) on the streamlines at different times for ϕ = 4%, Re = 100 and Pr = 6.2.

Fig. 6 shows the impact of varying the angular velocity of the finned cylinder on the isotherm contours for Re = 100, Pr = 6.2 and ϕ = 4%. Several time step units were chosen for this presentation to see how the heat transfer process takes place during the dimensionless time interval τ [0 - 200].

For Ω = -3, the rotation of the finned cylinder is clockwise, it is observed that just after the obstacle the thermal boundary layer near the bottom wall is thin while it is thick further in the channel downstream. For Ω = 5, counterclockwise rotation direction, the physical phenomenon is reversed and the thermal layer at the bottom wall is thick just after the obstacle and is much reduced towards the end of the channel. It is concluded that the enhancement is just after the obstacle when the direction of rotation is clockwise, while the enhanced part is towards the end of the channel when the rotation of the finned cylinder is counterclockwise. The region of heat transfer enhancement depends on the direction of the rotation of the finned cylinder.

For Ω = 0, when the heat transfer becomes stable from τ = 50, it is showed that the thermal boundary layer at the bottom wall is thickened due to the impact of the fin position on the cylinder following the reference of Toumi et al. (2022).

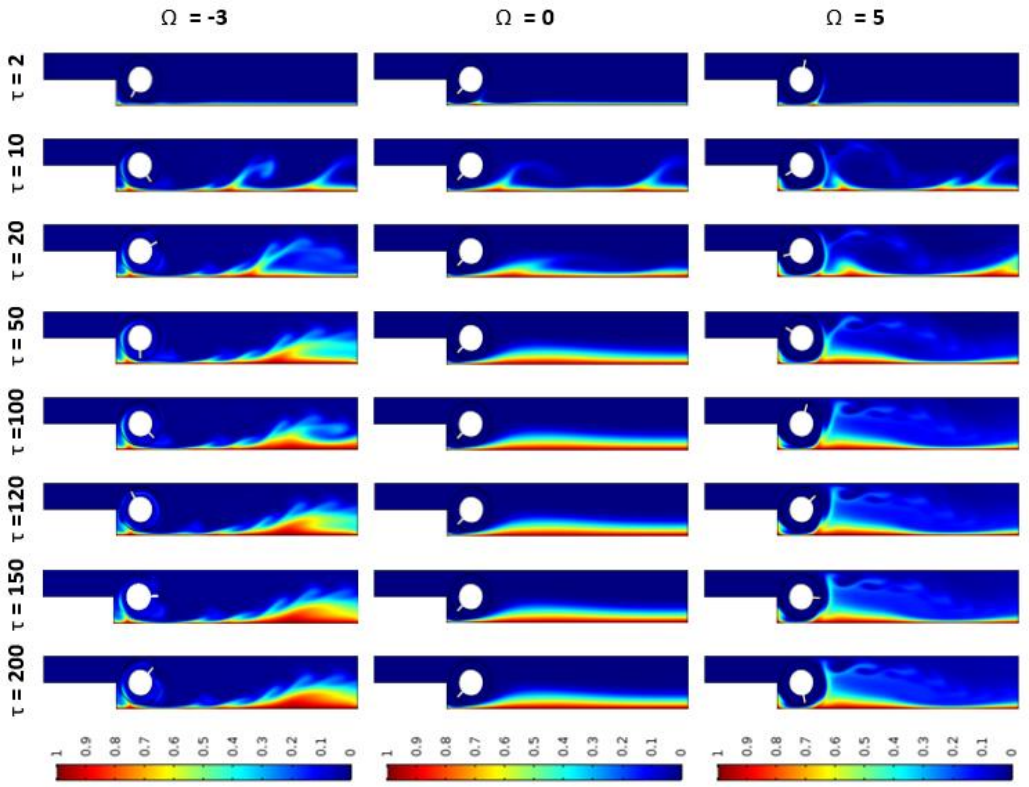

Fig. 6. Effect of the finned cylinder rotation (Ω) on the isotherms at different times for ϕ = 4%, Re = 100 and Pr = 6.2.

Quantitative results:

Many methods of heat transfer exist, including forced convection in heat transfer that occurs between a hot surface and cold fluid. The fluid is moved by an external force field (pump, fan, etc.). To measure the quality of heat transfer in the duct, the average Nusselt number and local Nusselt number are calculated.

The temporal evolution of the variation of the average Nusselt number over the duct surface and the local Nusselt number along the hot bottom wall for the two control parameters (rotation speed of the finned cylinder and Reynolds number) are presented in the figures below.

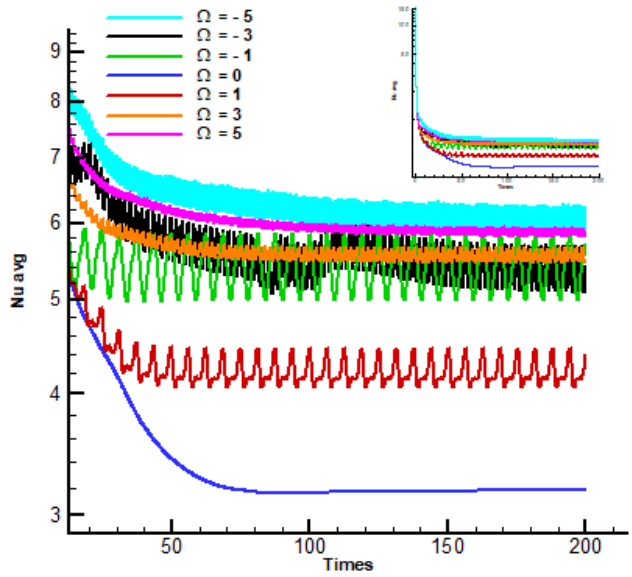

Fig. 7. Effect of the finned cylinder rotation (Ω) as a function of time on average Nusselt number for ϕ = 4%, Pr = 6.2 and Re = 100.

In the present paper, the main objective is to study the effect of the rotating finned cylinder. The dimensionless values of the angular velocity used to perform the unsteady numerical calculation are Ω = (-5, -3, -1, 0, 1, 3, 5) and the fixed values are Pr = 6.2, Re = 100 and ϕ = 4%.

In Fig. 7 a zoom of the temporal evolution of the average Nusselt number during the dimensionless time interval τ [0-200] is displayed. It is noticed that for the case of rotation in the same clockwise direction Ω = (-5, -3, -1), the amplitudes are more intense than in the case where the rotation is counterclockwise Ω = (1, 3, 5). The thermal amplitude temperature difference between the maximum and minimum is large when the values of Ω are negative causing instability of the flow. For the same values of rotational speed in both directions Ω = (-5, +5) and Ω = (-3, +3), the values of the average Nusselt number are close. In addition to the effect of rotation, it is worth mentioning the effect of the fin position on the excellent heat transfer quality (Toumi et al. 2022) who found an improvement of 27% for the case of Ω = 0 with finned cylinder compared to the finless cylinder of the work of (Shafqat Hussain and Sameh E. Ahmed 2019).

The rotation of the obstacle affects the heat transfer significantly. It takes the lowest values for the stationary obstacle case (fixed fin cylinder) and high values in the rotating cases. A 96% improvement difference is observed between a rotation speed of (Ω = -5, Nuavg = 6.24) and that of (Ω = 0, Nuavg = 3.18).

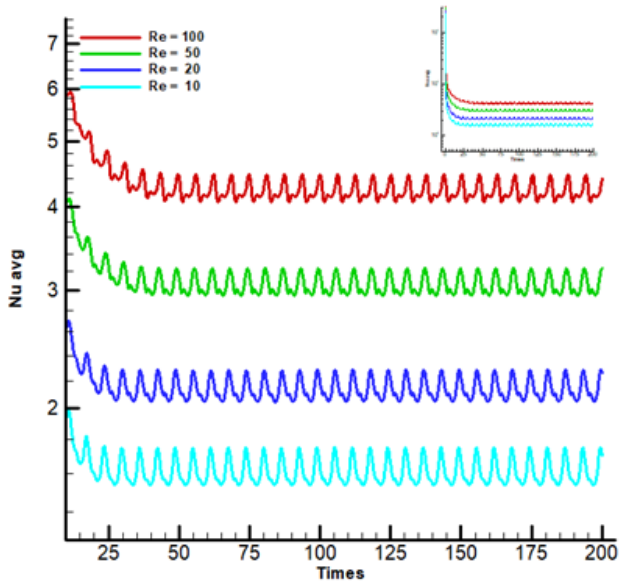

Fig. 8. Effect of Reynolds number as a function of time on average Nusselt number for $\phi = 4\%$, Pr = 6.2 and $\Omega = 1$.

A zoom of the temporal evolution of the mean Nusselt number under the effect of the Reynolds number (Re = 10, 20, 50, 100) in the interval τ [0-200] is shown in Fig. 8 with $\phi = 0.04$, Pr = 6.2 and $\Omega = 1$.

For low Reynolds number value (Re = 10) the quality of heat transfer is reduced and the average Nusselt number take the lowest value which reaches 1.70. On the other hand when Re = 100, the value of the average Nusselt is the highest and reaches 4.40. It is concluded that when the value of the Reynolds number increases, the mean Nusselt number increases as the increased inertial forces related to the velocities accelerate the motion of the nanofluid flow.

The thermal amplitude of the temperature difference between the highest and lowest value is also a result of the fin position when the cylinder rotates. The fin attached to the cylinder has its effect on the characteristics of nanofluid flow and on heat transfer according to (Toumi et al. 2022).

Fig. 9 represents the impact of the angular rotation speed (Ω = -5, -3, -1, 0, 1, 3, 5) of the finned cylinder on the averaged heat transfer rate, with $\phi = 4\%$, Re = 100 and Pr = 6.2, for different times (τ = 20, 50, 150, 200). It is observed that from dimensionless time τ = 50, the quality of heat transfer rate is stable. When the rotation velocity obstacle $\Omega = 0$ (stationary case), the average Nusselt values are minimal and with increasing angular velocity, the average Nusselt number also increases and takes maximum values for Ω = -5.

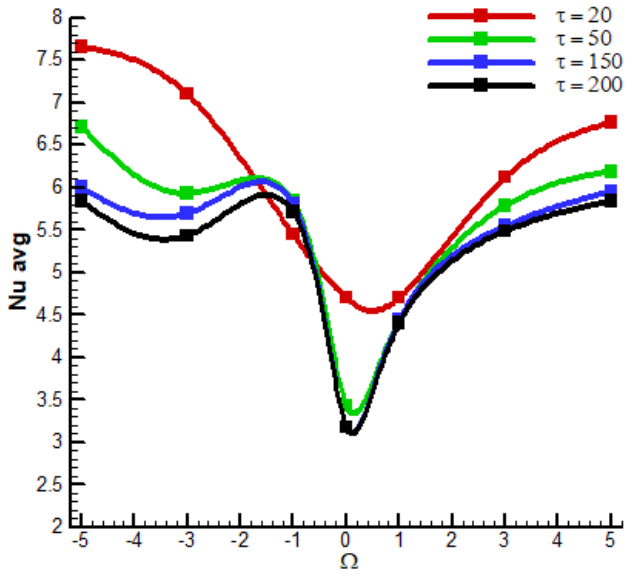

Fig. 9. Effect of the finned cylinder rotation (Ω) on average Nusselt number for ϕ = 4%, Re = 100 and Pr = 6.2 at various instants.

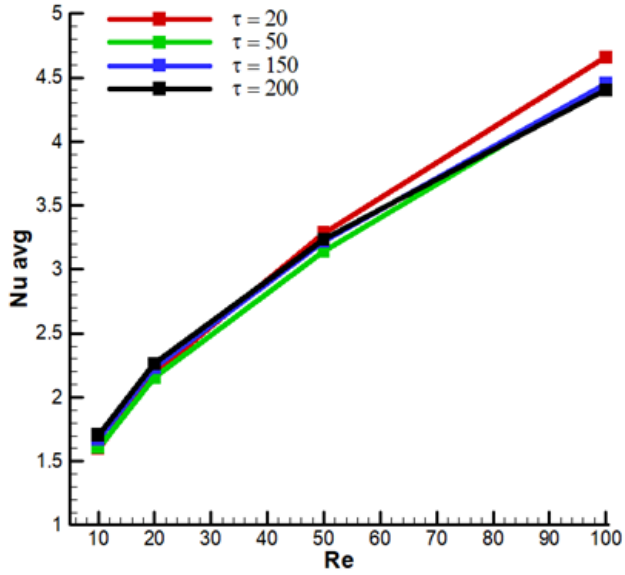

Fig. 10. Impact of the Reynolds number (Re) on average Nusselt number for Pr = 6.2, Ω = 1 and ϕ = 4% at various instants.

The influence of Reynolds number (Re = 10, 20, 50, 100) on the average Nusselt number for different times (τ = 20, 50, 150, 200) is presented in Fig. 10, with the fixed values Pr = 6.2, Ω =

1 and $\phi = 0.04$. It is clearly observed that when Reynolds number increases, the Nusselt number also increases under the impact of flow velocities. From the dimensionless time $\tau = 50$, the values of the average Nusselt number are almost identical because heat transfer is stable.

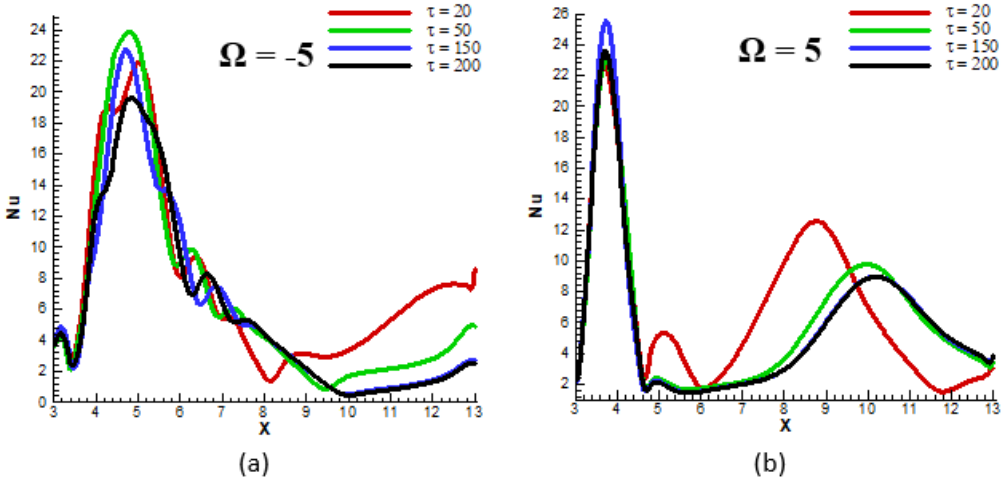

Fig. 11. Local Nusselt number distribution along the heated bottom wall at various times for Re = 100, $\phi = 4\%$, Pr = 6.2 and $\Omega = -5$ (a) & $\Omega = 5$ (b).

The local Nusselt number distribution on the bottom hot wall at different times ($\tau = 20$, 50, 150, 200) is presented in Fig. 11 for $\Omega = -5$ (a) and $\Omega = 5$ (b), with the fixed values $\phi = 0.04$, Re = 100 and Pr = 6.2. When the rotation is negative ($\Omega = -5$), the flow motion is unstable at the back of the obstacle and the value of the local Nusselt number are high at this location and then start to decrease towards the end of the duct. When the rotation is positive ($\Omega = 5$), the local Nusselt number values after and in the vicinity of the obstacle are low (from X = 4.8 to X = 8) and then they start to increase which improves the forced convection transfer at this region towards the end of the duct away from the finned cylinder. The cooling region for removing unwanted heat from the bottom wall depends on the direction of rotation.

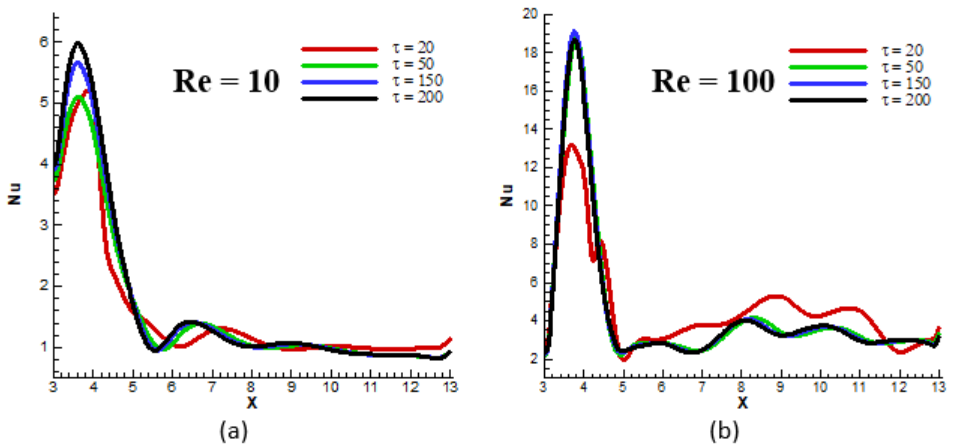

Fig. 12. Local Nusselt number distribution along the heated bottom wall at various times for $\phi = 4\%$, $\Omega = 1$, Pr = 6.2 and Re = 10 (a) & Re = 100 (b).

In Fig. 12, it is displayed the distribution of the local Nusselt number for several instants (τ = 20, 50, 150, 200), for two different Reynolds numbers, a low Reynolds in Fig. 12.a (Re = 10) and a Reynolds value of 100 in Fig. 12.b, with Pr = 6.2, Ω = 1 and ϕ = 0.04.

The peaks between X = 3 and X = 5, correspond to the lower part of the finned cylinder. A large gap is observed between the local Nusselt number peaks which corresponds to the two Reynolds values. The local Nusselt number peak for Reynolds number Re = 100 is three times larger than that for Reynolds number Re = 10.

For Re = 10, the local Nusselt number values are low and from X = 5.5 until the end of the duct they are in the vicinity of 1. This low forced convection is due to the low force of inertia which made the nanofluid motion slow. In Fig. 12.b and for Re = 100, the values of the local Nusselt number are high because the force of inertia is increased, which leads to an improved heat transfer.

5. Conclusions

In this paper, the effect of the rotating finned cylinder on the improvement of the heat transfer quality and on the characteristics of the nanofluid flow is studied. An unsteady numerical investigation was realized to analyze the effect of the angular rotation speed of the finned cylinder as a key control parameter. Different values for the angular velocity (Ω = -5, -3, -1, 0, 1, 3, 5) as well as the Reynolds number (Re = 10, 20, 50 and 100) were used. Conclusions are as follows:

- In all values of the control parameters of the simulation results, the flow of the nanofluid is at its complete thermal development from the dimensionless time unit τ = 50, except for the two values of rotational speed Ω = - 3 and Ω = -5.
- The convective heat transfer is significantly affected by the rotation of the obstacle and is strongly increased. It takes the lowest values for the stationary obstacle case (fixed fin cylinder) and high values in the rotating case.
- The cooling zone for removing unwanted heat from the bottom wall depends on the direction of rotation of the finned cylinder.
- A 96% improvement difference is observed between a rotation speed of (Ω = -5, Nuavg = 6.24) and that of fixed fin cylinder (Ω = 0, Nuavg = 3.18).
- A difference of 177.33% improvement is observed between a rotational speed of finned cylinder (present work) (Ω = -5, Nuavg = 6.24) and that of cylinder without fin (reference work of Hussain and Ahmed [12]) (Ω = 25, Nuavg = 2.25), while the rotational speed of the present work is five times less than that of Hussain and Ahmed [12].
- The temperature fluctuations are more intense when the value of Reynolds number increases from 50 to 100 and the mixing of cold nanofluid and hot fluid is improved.

Nomenclature

t	Time (s)		**Greek symbols**
T	temperature	ϕ	nanoparticle concentration
H	inlet step height,	τ	dimensionless time $\tau = t\,U_0/H$
Nu	local Nusselt number	α	thermal diffusivity

Nu_{avg}	averaged Nusselt number	ω	angular rotational velocity (rad/s)
Pr	Prandtl number	Ω	adimensional angular rotational velocity of finned cylinder
Re	Reynolds number	θ	adimensional temperature $T - T_c/T_h - T_c$
K	thermal conductivity	ρ	fluid density (kg/m^3)
h	Local heat transfer coefficient	μ	dynamic viscosity, N s/m^2
n	unit normal vector	ν	kinematic viscosity (m^2/s)
p	pressure	β	expansion coefficient
P	adimensional pressure	ψ	stream function
Cp	Thermal specific heat		**Subscripts**
u, v	x–y velocity components (m/s)	*avg*	average
x, y	Cartesian coordinates (m)	*f*	Basic fluid
U, V	adimensional velocity components	*nf*	nanofluid
X, Y	adimensional Cartesian coordinates	*h*	Hot temperature
		c	Cold temperature

References

Al-Aswadi A A, Mohammed H, AShuaib N H and Campo A (2010). Laminar forced convection flow over a backward facing step using nanofluids, International Communications in Heat and Mass Transfer. vol. 37, no 8, p. 950-957. doi.org/10.1016/j.icheatmasstransfer.2010.06.007

Costa V A F and Raimundo A M (2010). Steady mixed convection in a differentially heated square enclosure with an active rotating circular cylinder. International Journal of Heat and Mass Transfer, vol. 53, no 5-6, p. 1208-1219. doi.org/10.1016/j.ijheatmasstransfer.2009.10.007

Hilo A K, Iborra A A, Sultan M T H and Hamid M F A (2020). Experimental study of nanofluids flow and heat transfer over a backward-facing step channel. Powder Technology, vol. 372, p. 497-505. doi.org/10.1016/j.powtec.2020.06.013

Hussain S and Ahmed S E (2019). Unsteady MHD forced convection over a backward facing step including a rotating cylinder utilizing Fe3O4-water ferrofluid. Journal of Magnetism and Magnetic Materials, vol. 484, p. 356-366. doi.org/10.1016/j.jmmm.2019.04.040

Ikhtiar U, Manzoor S, Sheikh N A and Ali M (2016). Free stream flow and forced convection heat transfer around a rotating circular cylinder subjected to a single gust impulse. International Journal of Heat and Mass Transfer, vol. 99, p. 851-861. doi.org/10.1016/j.ijheatmasstransfer.2016.04.045

Kherbeet A S, Mohammed H A and. Salman B H (2012). The effect of nanofluids flow on mixed convection heat transfer over microscale backward-facing step. International Journal of Heat and Mass Transfer," vol. 55, no 21-22, p. 5870-5881. doi.org/10.1016/j.ijheatmasstransfer.2012.05.084

Kumar A and Dhiman A K (2012), Effect of a circular cylinder on separated forced convection at a backward-facing step. International Journal of Thermal Sciences, vol. 52, p. 176-185. doi.org/10.1016/j.ijthermalsci.2011.09.014

Lv J, Hu C, Bai M, Li L, Shi L, and Gao D (2019). Visualization of SiO2-water nanofluid flow characteristics in backward-facing step using PIV. Experimental Thermal and Fluid Science, vol. 101, p. 151-159. doi.org/10.1016/j.expthermflusci.2018.10.013

Mobadersani F and Rezavand Hesari A (2020), Magneto Hydrodynamic Effect on Nanofluid Flow and Heat Transfer in Backward-Facing Step Using Two-Phase Model. AUT Journal of Mechanical Engineering, vol. 4, no 1, p. 51-66. 10.22060/AJME.2019.14843.5747

Moosavi R, Moltafet R, Lin C X and Chuang P Y A (2021). Numerical modeling of fractional viscoelastic non-Newtonian fluids over a backward facing step–Buoyancy driven flow and heat transfer. Thermal Science and Engineering Progress. vol. 21, p. 100767. doi.org/10.1016/j.tsep.2020.100767

Nath R and Krishnan M (2019). Numerical study of double diffusive mixed convection in a backward facing step channel filled with Cu-water nanofluid. International Journal of Mechanical Sciences, vol. 153, p. 48-63. doi.org/10.1016/j.ijmecsci.2019.01.035

Rahman M M, Öztop H F, Mekhilef S, Saidur R and Al-Salem K (2014). Unsteady natural convection in Al2O3–water nanoliquid filled in isosceles triangular enclosure with sinusoidal thermal boundary condition on bottom wall. Superlattices and Microstructures, vol. 67, p. 181-196. doi.org/10.1016/j.spmi.2014.01.001

Roslan R, Saleh H, Hashim I (2012). Effect of rotating cylinder on heat transfer in a square enclosure filled with nanofluids. International Journal of Heat and Mass Transfer, vol. 55, no 23-24, p. 7247-7256. doi.org/10.1016/j.ijheatmasstransfer.2012.07.051

Sarkar S, Ganguly S, Biswas G and Saha P (2016). Effect of cylinder rotation during mixed convective flow of nanofluids past a circular cylinder. Computers & Fluids, vol. 127, p. 47-64. doi.org/10.1016/j.compfluid.2015.12.013

Selimefendigil F and Öztop H F (2013). Identification of forced convection in pulsating flow at a backward facing step with a stationary cylinder subjected to nanofluid. International Communications in Heat and Mass Transfer, vol. 45, p. 111-121. doi.org/10.1016/j.icheatmasstransfer.2013.04.016

Selimefendigil F and Öztop H F (2014). Effect of a rotating cylinder in forced convection of ferrofluid over a backward facing step. International Journal of Heat and Mass Transfer, vol. 71, p. 142-148. doi.org/10.1016/j.ijheatmasstransfer.2013.12.042

Selimefendigil F and Öztop H F (2015). Influence of inclination angle of magnetic field on mixed convection of nanofluid flow over a backward facing step and entropy generation. Advanced Powder Technology, vol. 26, no 6, p. 1663-1675. doi.org/10.1016/j.apt.2015.10.002

Selimefendigil F and Öztop H F (2015). Numerical investigation and reduced order model of mixed convection at a backward facing step with a rotating cylinder subjected to nanofluid. Computers & Fluids, vol. 109, p. 27-37. doi.org/10.1016/j.compfluid.2014.12.007

Selimefendigil F and Öztop H F (2018a). Magnetic field effects on the forced convection of CuO-water nanofluid flow in a channel with circular cylinders and thermal predictions using ANFIS. International Journal of Mechanical Sciences, vol. 146, p. 9-24. doi.org/10.1016/j.ijmecsci.2018.07.011

Selimefendigil F and Öztop H F (2018b). Mixed convection of nanofluids in a three dimensional cavity with two adiabatic inner rotating cylinders. International Journal of Heat and Mass Transfer, vol. 117, p. 331-343. doi.org/10.1016/j.ijheatmasstransfer.2017.09.116

Selimefendigil F and Öztop H F (2020). Hydro-thermal performance of CNT nanofluid in double backward facing step with rotating tube bundle under magnetic field. International Journal of Mechanical Sciences, vol. 185, p. 105876. doi.org/10.1016/j.ijmecsci.2020.105876

Shirani N, Toghraie D, and Rostami S (2021). Comparative study of mixed convection heat transfer of water–Cu nanofluid in an enclosure having multiple rotating circular cylinders

with different configurations and considering harmonic cylinders rotation. Journal of Thermal Analysis and Calorimetry, vol. 144, no 4, p. 1557-1570. doi.org/10.1007/s10973-020-09624-9

Sufyan M, Manzoor S and Sheikh N A (2015). Free stream flow and forced convection heat transfer across rotating circular cylinder in steady regime: effects of rotation, Prandtl number and thermal boundary condition. Journal of Mechanical Science and Technology, vol. 29, no 4, p. 1781-1797. doi.org/10.1007/s12206-015-0351-3

Toumi M, Bouzit M, Bouzit F and Mokhefi A (2022). MHD forced convection using ferrofluid over a backward facing step containing a finned cylinder. Acta Mechanica et Automatica, vol. 16, no 1. doi.org/10.2478/ama-2022-0009

Turkyilmazoglu M (2014). Nanofluid flow and heat transfer due to a rotating disk. Computers & Fluids, vol. 94, p. 139-146,. doi.org/10.1016/j.compfluid.2014.02.009

Xie W A and Xi G N (2022). Flow instability and heat transfer enhancement of unsteady convection in a step channel. Alexandria Engineering Journal, vol. 61, no 9, p. 7377-7391. doi.org/10.1016/j.aej.2022.01.007

Xie W A, Xi G N and Zhong M B (2017). Effect of the vortical structure on heat transfer in the transitional flow over a backward-facing step. International Journal of Refrigeration, vol. 74, p. 465-474. doi.org/10.1016/j.ijrefrig.2016.11.001

Yang H, Zhang W and Zhu Z (2019). Unsteady mixed convection in a square enclosure with an inner cylinder rotating in a bi-directional and time-periodic mode. International Journal of Heat and Mass Transfer, vol. 136, p. 563-580. doi.org/10.1016/j.ijheatmasstransfer.2019.03.041

Yoon H S, Seo J H, and Kim J H (2010). Laminar forced convection heat transfer around two rotating side-by-side circular cylinder. International Journal of Heat and Mass Transfer, vol. 53, no 21-22, p. 4525-4535. doi.org/10.1016/j.ijheatmasstransfer.2010.06.041